Multi-level feature extraction for skin lesion segmentation in dermoscopic images

Sina Khakabi[a,b,c], Paul Wighton[a,b,c], Tim K. Lee[a,b,c] and M. Stella Atkins[a,b]

[a]School of Computing Science, Simon Fraser University, Burnaby, B.C., Canada, V5A 1S6;
[b]Department of Dermatology and Skin Science, University of British Columbia, and Vancouver Coastal Health Research Institute, Vancouver, B.C., Canada, V5Z 4E8;
[c]Cancer Control Research Program, BC Cancer Agency, Vancouver, B.C., Canada, V5Z 4E6

ABSTRACT

This paper presents a novel approach in computer aided skin lesion segmentation of dermoscopic images. We apply spatial and color features in order to model the lesion growth pattern. The decomposition is done by repeatedly clustering pixels into dark and light sub-clusters. A novel tree structure based representation of the lesion growth pattern is constructed by matching every pixel sub-cluster with a node in the tree structure. This model provides a powerful framework to extract features and to train models for lesion segmentation. The model employed allows features to be extracted at multiple layers of the tree structure, enabling a more descriptive feature set. Additionally, there is no need for preprocessing such as color calibration or artifact disocclusion. Preliminary features (mean over RGB color channels) are extracted for every pixel over four layers of the growth pattern model and are used in association with radial distance as a spatial feature to segment the lesion. The resulting per pixel feature vectors of length 13 are used in a supervised learning model for estimating parameters and segmenting the lesion. A dataset containing 116 challenging images from dermoscopic atlases is used to validate the method via a 10-fold cross validation procedure. Results of segmentation are compared with six other skin lesion segmentation methods. Our method outperforms five other methods and performs competitively with another method. We achieve a per-pixel sensitivity/specificity of 0.890 and 0.901 respectively.

1. INTRODUCTION

Cutaneous malignant melanoma is one of the most frequent types of cancer in the world. In recent decades, the annual rate of its incidence has been increasing by 3%-7% in fair-skinned populations.[1,2] It is increasing faster than any other cancer in the world, and in 2008, melanoma was the sixth most common malignancy in men and the seventh in women.[2] Despite the lethality of the disease, if the malignant lesion is detected early, it can be cured without complication. Hence, there is a growing demand for computer-aided-diagnosis of melanoma to improve the diagnostic accuracy.

There are several different modalities to obtain images of skin lesions. Up until 1995 pigmented lesions were mainly examined by naked eye, therefore early automated skin lesion analysis methods were performed on these simple camera-captured images, the so-called 'clinical' images, which record the surface characteristics of a skin lesion.[3] Around 1995, dermoscopy (aka: dermatoscopy, epiluminescense microscopy (ELM), skin surface microscopy, incident light microscopy) became available and automated skin lesion analysis methods began using dermoscopic images for analysis. A Dermoscope (alt: Dermoscopy) is a non-invasive hand-held device which is using either polarized light or oil immersion to render the outermost layer of the skin (called stratum corneum) translucent. Today, most research in automated skin lesion analysis and diagnosis uses dermoscopic images.[3]

Skin lesion segmentation is an essential preprocessing step in most Automated Skin Lesion Diagnostic (ASLD) systems. The quality of the segmentation of the skin lesion can be increased significantly if the growth pattern of the lesion is modelled and incorporated properly.

The growth of a skin lesion can occur in two different phases: radial and vertical. Both malignant and benign lesions begin by growing radially. In this phase, a pigmented lesion is formed by nests of melanocytes, which synthesize the brown pigmentation called melanin. In the vertical growth phase the malignant melanocytes starts penetrating into dermis. This phase is a qualitative step in the development of malignant melanoma. Visually, melanin appears as various shades of colors as it penetrates different layers of skin. Melanin is dark brown in

Medical Imaging 2012: Computer-Aided Diagnosis, edited by Bram van Ginneken, Carol L. Novak,
Proc. of SPIE Vol. 8315, 83150E · © 2012 SPIE · CCC code: 1605-7422/12/$18 · doi: 10.1117/12.911664

Downloaded From: http://proceedings.spiedigitallibrary.org/ on 10/14/2012 Terms of Use: http://spiedl.org/terms

epidermis, tan near the dermoepidermal junction, and blue-gray in the dermis.[4] This 3-dimensional information can be captured in a magnified 2-dimensional digital image using a dermoscope. In this paper we use this spatial information to decompose the image and extract features for lesion segmentation.

2. PREVIOUS WORK

Lesion segmentation is defined as an assignment of binary labels from the label set $L = \{'lesion', 'background'\}$ to the pixels in the image. However, segmentation can also be defined as assigning a probability of belonging to 'lesion' or 'background' for every pixel.[5] The probability can easily be transformed to the binary version of segmentation by utilizing thresholding techniques and morphological operations.

Skin lesion segmentation is a crucial step in automated skin lesion analysis. The quality of the extracted lesion border plays an important role in the output quality of some methods[6,7] as these methods directly use the border for the feature extraction. Other methods may use segmentation to determine the region of interest (ROI) in the lesion for feature extraction.[8]

Most segmentation methods are histogram based methods.[9–15] The main technique in the histogram based segmentation is to use gray level or color level (in different color spaces) intensity thresholding. In some of these methods, user interaction is also used to increase the quality of segmentation.[11]

Active contours and vector flow snakes have been applied to segment skin lesions.[16–18] Behavior of the active contour model (snake) is governed by minimizing the energy function that contains internal terms (smoothness/tension) and image terms (gradient flow around the boundary).

Statistical region merging (SRM) is another approach which is used to segment the skin lesion in dermoscopic images.[19]

The combination of some of these methods in association with the supervised or unsupervised machine learning methods provided interesting results. Iyatomi et al. described a method called the dermatologist-like tumor extraction algorithm (DTEA)[20] which is based on thresholding followed by iterative region growing. In the J-image segmentation algorithm (JSEG)[21] which is provided by Celebi et al., the computational time is reduced by incorporating approximate lesion localization and searching the border neighborhood rather than the whole image. A multiscale region-growing method is then used to merge the resulting *J-images* into a final segmentation. Zhou et al. added a spatial constraint as a feature into cluster analysis of pixels and used k-means++ algorithm (KPP)[22] for segmenting the image.[23] The threshold fusion algorithm (FSN)[24] takes the results of several thresholding algorithms and fuses them using a Markov model to arrive at a final segmentation. Recently, Wighton et al. employed a supervised learning model to segment the lesion by learning the model parameters and computing the maximum likelihood over the pixels in the unseen images.[5] Random walker algorithm[25] is also employed to segment the skin lesion in dermoscopic images. In this method, the seed point properties for lesion and background pixels are learnt and used to fully automate the random walker algorithm for skin lesion segmentation. Tenenhaus et al.[26] used intensity values at multiple scales and logistic regression to segment images. They achieve an accuracy of 75%.

3. METHOD

3.1 Feature Extraction

Features are defined based on the color and the spatial data over the pixels of the image. Spatial and color features can be extracted simultaneously (see the two parallel pipelines in Fig. 1). For extracting the color features, the image is decomposed by repeatedly clustering pixels to model the growth pattern; then the color features are extracted based on the red, green and blue color channels over the layers of decomposition. A very preliminary spatial feature (radial distance) is also calculated for every pixel in parallel.

Downloaded From: http://proceedings.spiedigitallibrary.org/ on 10/14/2012 Terms of Use: http://spiedl.org/terms

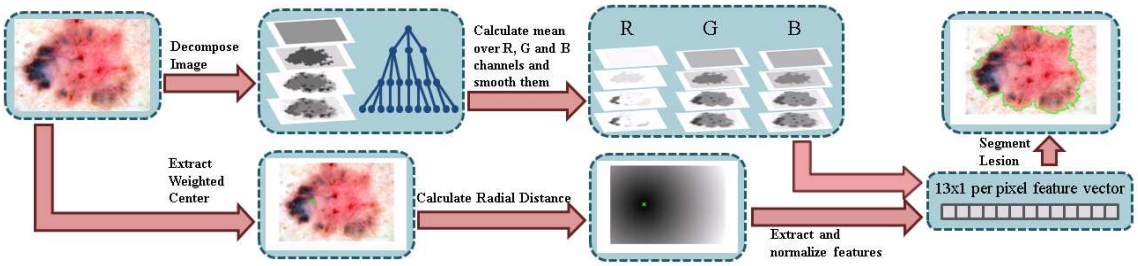

Figure 1. Overview of feature extraction procedure. Color based and space based features are extracted simultaneously and used in the segmentation algorithm.

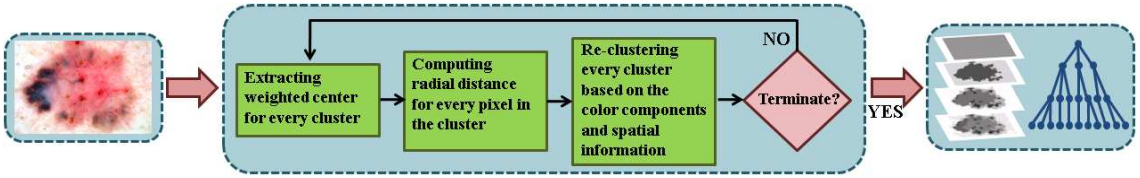

Figure 2. Flowchart of the image decomposition process

3.1.1 Extraction of Spatial Features

Extraction of weighted center of dark pixels: In contrast to Zhou et al.[23] who make the assumption that the center of the lesion the same as the center of the image, we provide a more general statement: the lesion center should be calculated with respect to the position of the dark spots over the lesion. This is calculated by taking specific number of dark pixels in the image and calculating a weighted average of coordinates of these pixels. The center obtained in this way can be interpreted as the center of the growth of the lesion. We use the following equation for calculating the center point coordinate:

$$x_C = \frac{1}{N} \times \sum_{i=1}^{N} x_i \text{ and } y_C = \frac{1}{N} \times \sum_{i=1}^{N} y_i \tag{1}$$

where $N = |X| = |Y|$. Simply, (x_C, y_C) is the centroid of the dark pixels.

Computing radial distance: Radial distance is a feature computed for every pixel based on its distance from the calculated center point; therefore, for a specific pixel we set this value to the Euclidean distance between the center point and the pixel as follows:

$$D_{x,y} = \sqrt{(x - x_C)^2 + (y - y_C)^2} \tag{2}$$

where $D_{x,y}$ is the radial distance computed for the pixel in position (x, y).

3.1.2 Image Decomposition and Extraction of Color Based Features

Extraction of the color based features is done on a multi-scale tree-structured model of the lesion growth pattern. We build this model by performing three steps as presented in Fig. 2. These three steps are repeated four times resulting in a tree-structure with four layers. The first two steps are similar to the section 3.1.1, although, these steps are repeated for every resulting sub-cluster.

Clustering stage: In the first iteration there is only one cluster containing all pixels of the image. Color features for clustering stage are set to green and blue channel from RGB color-space. Red channel is eliminated in order to reduce the effect of the blood vessels in the clustering stage. Therefore, by adding radial distance (RD) to the feature set in the clustering stage, the feature set $\{G, B, RD\}$ is obtained. These features are used in $k - means$[27] clustering algorithm to cluster pixels into two (dark and light) clusters at every iteration. In the following iteration, every cluster is re-clustered to dark and light clusters and this is repeated four times. In this stage, for every disjoint cluster we add a corresponding node to the tree structure. Thus, the root in the

Downloaded From: http://proceedings.spiedigitallibrary.org/ on 10/14/2012 Terms of Use: http://spiedl.org/terms

Method	AUC	Sens.	Spec.	ΔAUC	ΔSens.	ΔSpec.
Our method	0.956	0.890	0.901	N/A	N/A	N/A
G-LoG/LDA	0.948	0.880	0.887	0.008	0.010	0.014
KPP	N/A	0.717	0.790	N/A	0.164	0.025
DTEA	N/A	0.641	0.987	N/A	0.035	-0.001
SRM	N/A	0.770	0.946	N/A	0.002	0.024
JSEG	N/A	0.678	0.986	N/A	-0.002	-0.001
FSN	N/A	0.812	0.935	N/A	0.012	0.017

Table 1. Comparison of results of our method with other six methods.

tree corresponds to a cluster containing all pixels of the image. The second layer contains two groups of nodes corresponding to light and dark clusters. This structure is retained through four layers of the tree. This tree structure has two important properties: *i*) summation of the pixels at every layer of the tree is equal to the number of pixels in the image, and *ii*) every pixel belongs to exactly one cluster at every layer of the tree. These two properties of the tree lead to a novel approach in extraction of the features for the lesion segmentation task. Decomposing the image into such a tree-structure provides a rich description over which many salient features can be extracted.

Feature extraction: We use some preliminary, but powerful features for lesion segmentation task. First, the average of red, green, and blue intensity channels is calculated in every cluster. In the next step, mean values are blurred by a 15×15 Gaussian filter with $\sigma = 5$. For every pixel, the corresponding values from every color channel in every layer of the tree is extracted and used to construct the feature vector of length 12. Full details are given in.[28]

3.2 Supervised Learning Based Segmentation

The feature vector of length 13 is obtained by adding radial distance to the group of 12 color based feaures. Extracted feature vectors are used to segment the skin lesion using a general supervised learning model for ASLD. 10-fold cross validation is used for testing all segmentation methods. The details of the model can be found in Khakabi et al.'s MSc thesis[28] and Wighton et al.'s paper.[5]

4. RESULTS

We present some segmentation results and compare them to six other skin lesion segmentation techniques: G-LoG/LDA,[5] KPP,[23] JSEG,[21] DTEA,[20] SRM,[19] and FSN.[24] We have used the authors' implementation of their methods on the same dataset to evaluate results.

A dataset containing 116 challenging images from dermoscopic atlases[4,29] is used. Some examples of segmentation results are provided in Fig. 3.

Similar to G-LoG/LDA, the output of the provided method is a probability map of the pixels in the lesion. Consequently, by changing the threshold of the segmentation over this probability map the ROC curves are obtained (see Fig. 4). The output of other five methods is binary segmentation of lesions; therefore, we use the nearest point on the ROC curve to compare the sensitivity/specificity pairs (see Table 1). In this table, ΔSens. and ΔSpec. are the difference between the sensitivity/specificity of methods with the closest pair on ROC curve.

Our method outperforms G-LoG/LDA, KPP, DTEA, SRM, and FSN, and is comparable to JSEG's performance.

5. CONCLUSION AND FUTURE WORK

In this work, a novel approach for feature extraction based on decomposition of dermoscopic images has been presented. Although extracted features in this framework are preliminary, competitive performance is obtained. In addition, an important property of this method is that it performs well even without applying the preprocessing steps such as color calibration and hair and noise removal. Additional improvement to this method could be

Downloaded From: http://proceedings.spiedigitallibrary.org/ on 10/14/2012 Terms of Use: http://spiedl.org/terms

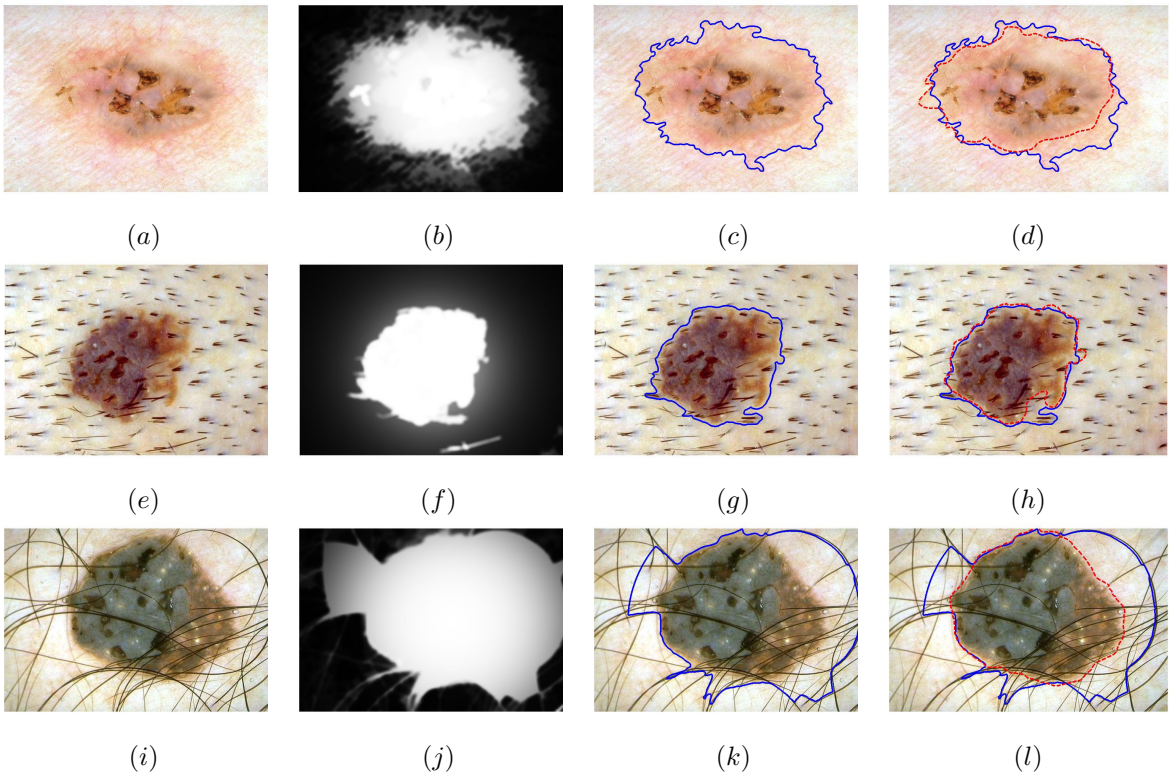

Figure 3. Example of challenging images for segmentation. (a), (e) and (i) are original dermoscopic images, (b), (f) and (j) are probability maps obtained using the learning model, (c), (g) and (k) are our segmentation results, and (d), (h) and (l) are provided for comparison with the ground-truth segmentations (red dashed lines).

obtained using well defined features and further decomposition of the image to lower layers that will result in smoother pixel probability maps.

REFERENCES

[1] Marks, R., "Epidemiology of melanoma," *Clinical and Experimental Dermatology* **25**(6), 459–463 (2000).

[2] Erickson, C. and Driscoll, M. S., "Melanoma epidemic: Facts and controversies," *Clinics in Dermatology* **28**(3), 281–286 (2010).

[3] Day, G. and Barbour, R., "Automated melanoma diagnosis: where are we at?," *Skin Research and Technology* **6**(1), 1–5 (2000).

[4] Argenziano, G., Soyer, H. P., et al., "Dermoscopy of pigmented skin lesions: Results of a consensus meeting via the internet," *Journal of the American Academy of Dermatology* **48**(5), 679 – 693 (2003).

[5] Wighton, P., Lee, T. K., Lui, H., McLean, D. I., and Atkins, M. S., "Generalizing common tasks in automated skin lesion diagnosis," *IEEE Transactions on Information Technology in BioMedicine* (2011).

[6] Betta, G., Di Leo, G., Fabbrocini, G., Paolillo, A., and Scalvenzi, M., "Automated application of the 7-point checklist diagnosis method for skin lesions: Estimation of chromatic and shape parameters.," in [*IEEE Instrumentation and Measurement Technology Conference*], **3**, 1818 – 1822 (2005).

[7] Lee, T. K., McLean, D. I., and Atkins, M. S., "Irregularity index: A new border irregularity measure for cutaneous melanocytic lesions," *Medical Image Analysis* **7**(1), 47–64 (2003).

[8] Maglogiannis, I. and Doukas, C., "Overview of advanced computer vision systems for skin lesions characterization," *Information Technology in Biomedicine, IEEE Transactions on* **13**(5), 721 –733 (2009).

[9] Deng, Y. and Manjunath, B., "Unsupervised segmentation of color-texture regions in images and video," *IEEE Transactions on Pattern Analysis and Machine Intelligence* , 800–810 (2001).

Downloaded From: http://proceedings.spiedigitallibrary.org/ on 10/14/2012 Terms of Use: http://spiedl.org/terms

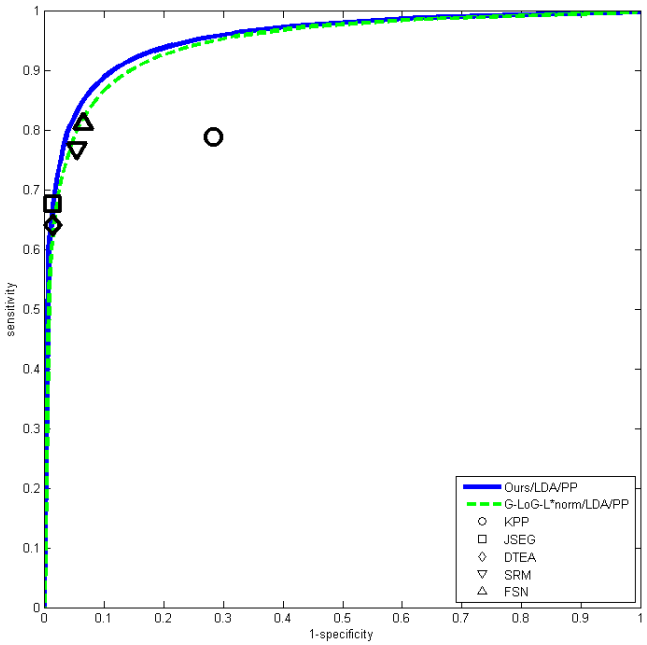

Figure 4. ROC curve demonstrating our method's segmentation results compared with six other methods: G-LoG/LDA,[5] KPP,[23] JSEG,[21] DTEA,[20] SRM,[19] and FSN.[24]

[10] Celebi, M., Kingravi, H., Uddin, B., Iyatomi, H., Aslandogan, Y., Stoecker, W., and Moss, R., "A methodological approach to the classification of dermoscopy images," *Computerized Medical Imaging and Graphics* **31**(6), 362–373 (2007).

[11] Ganster, H., Pinz, P., Rohrer, R., Wildling, E., Binder, M., and Kittler, H., "Automated melanoma recognition," *Medical Imaging, IEEE Transactions on* **20**(3), 233–239 (2001).

[12] Green, A., Martin, N., Pfitzner, J., O'Rourke, M., and Knight, N., "Computer image analysis in the diagnosis of melanoma+," *Journal of the American Academy of Dermatology* **31**(6), 958–964 (1994).

[13] Schmid-Saugeon, P., Guillod, J., and Thiran, J., "Towards a computer-aided diagnosis system for pigmented skin lesions," *Computerized Medical Imaging and Graphics* **27**(1), 65–78 (2003).

[14] Xu, L., Jackowski, M., Goshtasby, A., Roseman, D., Bines, S., Yu, C., Dhawan, A., and Huntley, A., "Segmentation of skin cancer images," *Image and Vision Computing* **17**(1), 65–74 (1999).

[15] Zagrouba, E. and Barhoumi, W., "A prelimary approach for the automated recognition of malignant melanoma," *Image Analysis and Stereology Journal* **23**(2), 121–135 (2004).

[16] Taouil, K. and Romdhane, N., "Automatic segmentation and classification of skin lesion images," in [*Distributed Frameworks for Multimedia Applications, 2006. The 2nd International Conference on*], 1–12, IEEE (2006).

[17] Erkol, B., Moss, R., Joe Stanley, R., Stoecker, W., and Hvatum, E., "Automatic lesion boundary detection in dermoscopy images using gradient vector flow snakes," *Skin Research and Technology* **11**(1), 17–26 (2005).

[18] Sapiro, G., "Segmenting skin lesions with partial-differential-equations-based image processing algorithms," *Medical Imaging, IEEE Transactions on* **19**(7), 763–767 (2000).

[19] Celebi, M. et al., "Border detection in dermoscopy images using statistical region merging," *Skin Research and Technology* **14**(3), 347–353 (2008).

[20] Iyatomi, H. et al., "An improved internet-based melanoma screening system with dermatologist-like tumor area extraction algorithm," *Computerized Medical Imaging and Graphics* **32**(7), 566–579 (2008).

[21] Emre Celebi, M., Alp Aslandogan, Y., Stoecker, W., Iyatomi, H., Oka, H., and Chen, X., "Unsupervised border detection in dermoscopy images," *Skin Research and Technology* **13**(4), 454–462 (2007).

[22] Arthur, D. and Vassilvitskii, S., "k-means++: The advantages of careful seeding," in [*Proceedings of the eighteenth annual ACM-SIAM symposium on Discrete algorithms*], 1027–1035, Society for Industrial and Applied Mathematics (2007).

Downloaded From: http://proceedings.spiedigitallibrary.org/ on 10/14/2012 Terms of Use: http://spiedl.org/terms

[23] Zhou, H. et al., "Spatially constrained segmentation of dermoscopy images," in [*5th IEEE International Symposium on Biomedical Imaging: From Nano to Macro, ISBI 2008.*], 800–803 (2008).

[24] Celebi, M., Hwang, S., Iyatomi, H., and Schaefer, G., "Robust border detection in dermoscopy images using threshold fusion," in [*17th IEEE International Conference on Image Processing (ICIP)*], 2541–2544 (2010).

[25] Wighton, P., Sadeghi, M., Lee, T., and Atkins, M., "A fully automatic random walker segmentation for skin lesions in a supervised setting," *Medical Image Computing and Computer-Assisted Intervention–MICCAI 2009* , 1108–1115 (2009).

[26] Tenenhaus, A., Nkengne, A., Horn, J., Serruys, C., Giron, A., and Fertil, B., "Detection of melanoma from dermoscopic images of naevi acquired under uncontrolled conditions," *Skin Research and Technology* **16**(1), 85–97 (2010).

[27] Lloyd, S., "Least squares quantization in pcm," *Information Theory, IEEE Transactions on* **28**(2), 129–137 (1982).

[28] KhakAbi, S., "Tree-structure based framework for automated skin lesion analysis," (August 2011).

[29] Argenziano, G., Soyer, H. P., et al., [*Interactive Atlas of Dermoscopy (Book and CD-ROM)*], Edra Medical Publishing and New Media (2000).

Downloaded From: http://proceedings.spiedigitallibrary.org/ on 10/14/2012 Terms of Use: http://spiedl.org/terms